FBH1 promotes DNA double-strand breakage and apoptosis in response to DNA replication stress

Yeon-Tae Jeong,[1] Mario Rossi,[1] Lukas Cermak,[1,2] Anita Saraf,[3] Laurence Florens,[3] Michael P. Washburn,[3,4] Patrick Sung,[5] Carl Schildkraut,[6] and Michele Pagano[1,2]

[1]Department of Pathology, NYU Cancer Institute, New York University School of Medicine, [2]Howard Hughes Medical Institute, New York, NY 10016
[3]The Stowers Institute for Medical Research, Kansas City, MO 64110
[4]Department of Pathology and Laboratory Medicine, The University of Kansas Medical Center, Kansas City, KS 66160
[5]Department of Molecular Biophysics and Biochemistry, Yale University School of Medicine, New Haven, CT 06520
[6]Albert Einstein College of Medicine, Bronx, NY 10461

Proper resolution of stalled replication forks is essential for genome stability. Purification of FBH1, a UvrD DNA helicase, identified a physical interaction with replication protein A (RPA), the major cellular single-stranded DNA (ssDNA)–binding protein complex. Compared with control cells, FBH1-depleted cells responded to replication stress with considerably fewer double-strand breaks (DSBs), a dramatic reduction in the activation of ATM and DNA-PK and phosphorylation of RPA2 and p53, and a significantly increased rate of survival. A minor decrease in ssDNA levels was also observed. All these phenotypes were rescued by wild-type FBH1, but not a FBH1 mutant lacking helicase activity. FBH1 depletion had no effect on other forms of genotoxic stress in which DSBs form by means that do not require ssDNA intermediates. In response to catastrophic genotoxic stress, apoptosis prevents the persistence and propagation of DNA lesions. Our findings show that FBH1 helicase activity is required for the efficient induction of DSBs and apoptosis specifically in response to DNA replication stress.

Introduction

One of the most common and dangerous lesions facing a proliferating cell is a stalled or collapsed replication fork. Cells respond to this form of genotoxic stress by either repairing the damaged DNA or inducing apoptosis. Failures to respond correctly may result in genome instability and the propagation of deleterious mutations.

FBH1 (also called FBXO18 or FBX18) is a member of the UvrD family of DNA helicases and exhibits DNA-dependent ATPase and DNA-unwinding activities in the 3′ to 5′ direction (Kim et al., 2002, 2004). In addition, FBH1 contains an F-box domain and forms an SCF ubiquitin ligase complex (Kim et al., 2004; Sakaguchi et al., 2008; Lawrence et al., 2009). FBH1 homologues that contain both the helicase and F-box domains are present in *Schizosaccharomyces pombe* and vertebrates, but they are absent in a number of other model organisms, such as budding yeast, worms, and fly (Park et al., 1997; Kim et al., 2004). Deletion of *fbh1* in fission yeast leads to moderately increased sensitivity to DNA-damaging agents and spontaneous Rad51 focus formation. In addition, Fbh1 is essential for viability in the absence of either the RecQ DNA helicase Rqh1 (the orthologue of mammalian BLM) or the UvrD DNA helicase Srs2 (Morishita et al., 2005; Osman et al., 2005; Sakaguchi et al., 2008). This synthetic lethality is suppressed by deletion of the *rad51* paralogues, which are necessary to find homologous sequences on the sister chromatid and promote DNA strand invasion to initiate the repair of DNA damage via homologous recombination (HR). In summary, *S. pombe* Fbh1 limits the assembly of Rad51 nucleofilaments via its helicase activity.

The Rad51 inhibitory activity of *S. pombe* Fbh1 suggests an anti-HR activity similar to the Srs2 helicase in *Saccharomyces cerevisiae*. Because human FBH1 expression is able to rescue certain HR defects in *SRS2* mutant yeast, it was proposed that vertebrate FBH1 is the functional equivalent of yeast Srs2 (Chiolo et al., 2007). However, this hypothesis is in conflict with the presence of both Fbh1 and Srs2 in *S. pombe* (with only

Correspondence to Michele Pagano: michele.pagano@nyumc.org

Abbreviations used in this paper: DSB, double-strand break; HR, homologous recombination; HU, hydroxyurea; RPA, replication protein A; ssDNA, single-stranded DNA.

The Rockefeller University Press $30.00
J. Cell Biol. Vol. 200 No. 2 141–149
www.jcb.org/cgi/doi/10.1083/jcb.201209002

partially redundant functions) and the fact that other mammalian helicases and factors are also able to suppress HR in a manner similar to Srs2 (Barber et al., 2008; Chu and Hickson, 2009; Moldovan et al., 2012).

Vertebrate FBH1 function appears to differ substantially from *S. pombe* Fbh1 function. *FBH1*-null DT40 chicken cells display a modest increase in sister chromatid exchange (SCE) rates, but they do not display increased sensitivity to DNA damage or defects in repair by HR (Kohzaki et al., 2007). In human cells, exogenous FBH1 is recruited to genotoxic stress-induced single-stranded DNA (ssDNA), promotes ssDNA generation, and limits the association of RAD51 with chromatin in a helicase-dependent manner (Fugger et al., 2009). Moreover, FBH1 silencing moderately increases the SCE rate and the number of spontaneous Rad51 foci in S phase (Fugger et al., 2009). *Fbh1*$^{-/-}$ ES cells display a moderate increase in Rad51 localization to DNA damage sites, but they do not display HR defects or sensitivity to DNA damaging agents (Laulier et al., 2010). Instead, after Top2 inhibitor-induced decatenation stress, *Fbh1*$^{-/-}$ cells displayed multi-lobed nuclei, micronuclei, and substantial defects in separation of anaphase chromosomes.

Therefore, although fission yeast Fbh1 restrains HR and inhibits the association of Rad51 with damaged DNA, data from vertebrate systems suggest only a minor or redundant role for FBH1 in HR, leaving much of FBH1 function a mystery.

The replication protein A (RPA) complex, consisting of the RPA1, RPA2, and RPA3 subunits, is the major ssDNA-binding complex in eukaryotes. During DNA replication, RPA prevents ssDNA from annealing with a complementary strand or forming secondary structures. Significant lengths of ssDNA are generated either after nucleolytic processing of a DSB or during DNA replication stress, which uncouples the replicative DNA helicase from the DNA-polymerase machinery. RPA stabilizes ssDNA regions and generates a platform for the recruitment of additional proteins essential for the activation of the ATR-CHK1 signaling cascade (Ciccia and Elledge, 2010).

In response to DNA replication stress, RPA2 is phosphorylated by ATR on Ser33. If replication stress persists, DSBs are generated (Petermann et al., 2010; Saintigny et al., 2001), resulting in the activation of other DNA damage–dependent kinases (ATM and DNA-PK) and the further phosphorylation of RPA2 on Ser4 and Ser8 by DNA-PK. Overall, it appears that RPA2 phosphorylation redirects RPA functions from DNA replication to DNA repair or apoptosis signaling (Binz et al., 2004; Manthey et al., 2007).

The study described herein demonstrates an interaction between FBH1 and RPA and elucidates a critical role for FBH1 in the response to DNA replication stress.

Results and discussion

The helicase domain of FBH1 is required for the efficient phosphorylation of RPA2 on Ser4 and Ser8 in response to replication stress

To identify FBH1 interactors, FLAG-HA–tagged FBH1 was transiently expressed in HeLa or HEK-293T cells and immunopurified for analysis by multidimensional protein identification technology (MudPIT; Florens and Washburn, 2006), which revealed peptides corresponding to RPA1, RPA2, and RPA3 (Tables S1 and S2). To investigate whether the binding between the RPA complex and FBH1 is specific, we screened a panel of 14 FBXO-family proteins, which includes FBH1, for interactions with the RPA complex by transient expression in HEK-293T cells and immunoprecipitations. We found that only FBH1 was able to coimmunoprecipitate endogenous RPA1, RPA2, and RPA3 (Fig. 1 A and unpublished data).

Because the RPA complex binds ssDNA, we induced long stretches of ssDNA in U2OS cells with hydroxyurea (HU), which blocks ribonucleotide reductase (RNR), resulting in deoxyribonucleotide depletion and rapid stalling of DNA replication forks. First, we noticed that FBH1 was progressively recruited to the chromatin fraction after HU treatment (Fig. 1 B). We then determined the effects of FBH1 knockdown on the localization of RPA2 to chromatin using three different siRNA oligos that do not affect the cell cycle or DNA synthesis (Fig. 1 C; Fig. S1 A; and unpublished data). We found that silencing of FBH1 reduced the amount of RPA2 in the chromatin fraction of U2OS cells exposed to HU (Fig. 1 B). Taking into account the reduction in total RPA2, FBH1 depletion did not affect the amount of Ser33-phosphorylated RPA2 [p-RPA2(S33)], as shown by both immunoblotting and immunofluorescence (Fig. 1, B and D). In contrast, the amount of Ser4- and Ser8-phosphorylated RPA2 [p-RPA2(S4/S8)] dramatically decreased when FBH1 was depleted (Fig. 1, B and C). Virtually identical results were obtained in nontransformed, nonimmortalized, diploid human fibroblasts (Fig. S1 B). The reduction in p-RPA2(S4/S8) in FBH1-depleted cells was also observed when replication stress was induced with gemcitabine, an RNR inhibitor used in the clinic, but not when genotoxic stress was induced with either neocarzinostatin, camptothecin, or adriamycin (Fig. S1, C and D; and unpublished data).

We then investigated which domain in FBH1 promotes the phosphorylation of Ser4 and Ser8. The effect of FBH1 silencing on p-RPA2(S4/S8) was rescued by expressing near-physiological levels of wild-type, siRNA-insensitive FBH1 (Fig. S2, A and B; and Fig. 2 A). Similar results were obtained using FBH1(PIP) (a PCNA-binding mutant; Fig. S2 C), FBH1(LPAA) (a SKP1-binding mutant; Fugger et al., 2009), and FBH1(S107/634A) (a mutant in which two putative ATM/ATR sites, Ser107 and Ser634, were mutated to Ala). In contrast, FBH1(D698N), a helicase domain mutant (Fugger et al., 2009), was unable to rescue the phosphorylation of RPA2 on Ser4 and Ser8 (Fig. 2 A; Fig. S2, A–C). Interestingly, FBH1(D698N) failed to bind RPA, although it interacted with SKP1 and CUL1 (Fig. S2 D).

After HU treatment, FBH1 induces DSBs and activation of ATM and DNA-PK

The persistence of RPA2 Ser33 phosphorylation and accompanying decrease in Ser4 and Ser8 phosphorylation after HU treatment suggested that fewer DSBs are generated in cells depleted of FBH1 compared with control cells, and this prediction was verified using neutral comet assays, which specifically detect DSBs (Fig. 2 B). Accordingly, compared with control cells, although FBH1 knockdown cells showed similar levels of CHK1

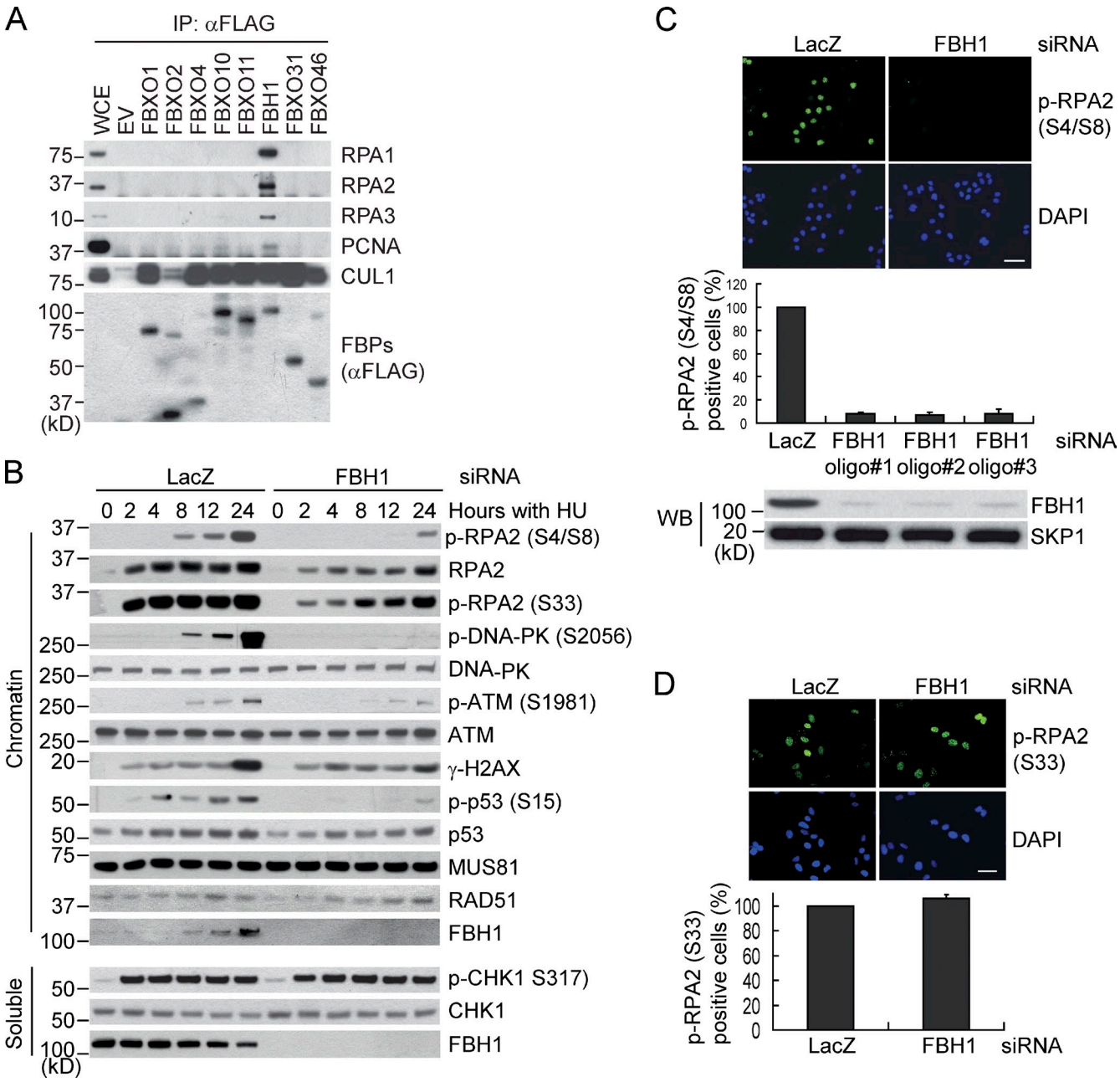

Figure 1. **FBH1 is required for the efficient activation of ATM and DNA-PK after DNA replication stress.** (A) HEK-293T cells were transfected with the indicated FLAG-tagged F-box proteins (FBPs) or an empty vector (EV). 24 h after transfection, cells were harvested and lysed. Whole-cell extracts (WCE) were subjected to immunoprecipitation (IP) with α-FLAG resin and immunoblotted as indicated. (B) U2OS cells were transfected with siRNAs against either LacZ or *FBH1* mRNA. After 48 h, cells were treated with HU for the indicated times. After harvesting, cells were fractionated into soluble and chromatin fractions, and lysates were immunoblotted as indicated. (C) U2OS cells were transfected with siRNAs to either LacZ or *FBH1* mRNA (in the latter case using three different oligos). 48 h after transfection, cells were treated with HU for 24 h and stained as indicated. Bar, 50 µm. The percentage of S-phase cells (i.e., RPA2-positive cells) that were also positive for p-RPA2(S4/S8) from three different experiments was plotted graphically (±SD). (D) U2OS cells were transfected with siRNAs to either LacZ or *FBH1* mRNA. 48 h after transfection, cells were treated with HU for 24 h and stained as indicated. Bar, 50 µm. The number of p-RPA2(S33)–positive cells from three different experiments was plotted graphically (±SD).

Ser317 phosphorylation (indicative of active ATR), they displayed a dramatic reduction in the activation of ATM and DNA-PK, as determined by examining the phosphorylation status of Ser1981 and Ser2056, respectively (Figs. 1 B, 2 C, and S1 B). Additionally, p53, a substrate of ATM and DNA-PK, was much less phosphorylated on Ser15 and accumulated less in FBH1-depleted cells (Fig. 1 A and Fig. S1 B). These experiments show that FBH1 is required for efficient DSB formation and the consequent induction of the DSB signaling cascade.

Rescue experiments with siRNA-insensitive constructs encoding wild-type FBH1 and the FBH1(D698N) mutant demonstrated that the helicase domain of FBH1 is required for DSB formation (as assessed by a neutral comet assay) and the activation of ATM and DNA-PK (Fig. 2, C and D).

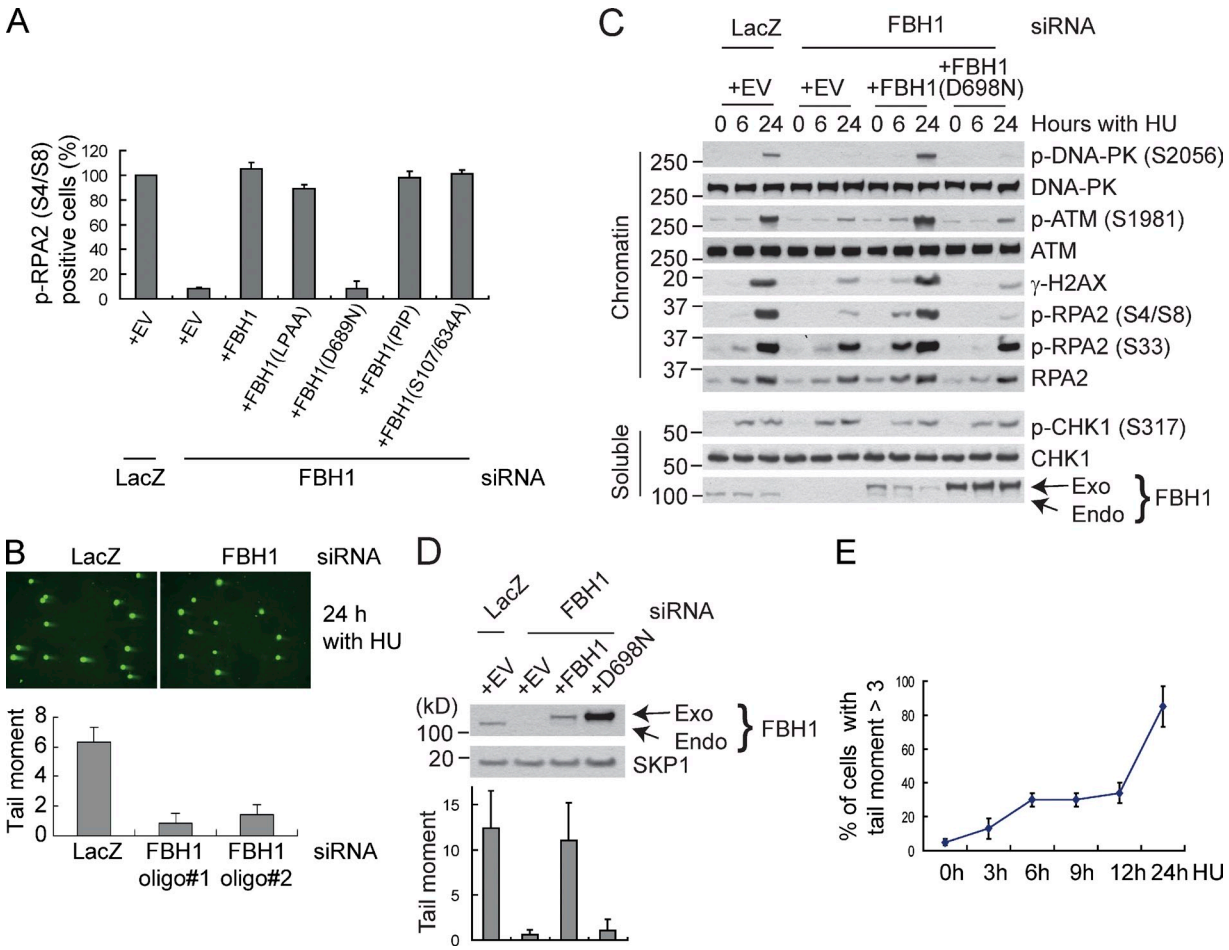

Figure 2. **The helicase domain of FBH1 is required for DSB formation and signaling.** (A) U2OS cells stably infected with either an empty vector (EV), wild-type FBH1, or the indicated FBH1 mutants were transfected with siRNAs to either LacZ or *FBH1* mRNA. After 48 h, cells were treated with HU for an additional 24 h and the number of p-RPA2(S4/S8)–positive cells from three different experiments was determined and plotted graphically (±SD). (B) U2OS cells were transfected with siRNAs to either LacZ or *FBH1* mRNA (in the latter case using two different oligos). After 48 h, cells were treated with HU for an additional 24 h and analyzed for the presence of DSBs using a neutral comet assay. Representative images are shown. The means (±SD) of at least three independent experiments are shown in the graph below. (C) U2OS cell lysates from an experiment performed in A were immunoblotted for the indicated proteins, including both endogenous (Endo) and exogenous (Exo) FBH1. (D) U2OS cells stably infected with either an empty vector (EV), wild-type FBH1, or FBH1(D698N) were transfected with siRNAs to either LacZ or *FBH1* mRNA. After 48 h, cells were treated with HU for 24 h and immunoblotted for SKP1 (loading normalization) and both endogenous (Endo) and exogenous (Exo) FBH1. The bottom graph shows the corresponding analysis of DSBs using a neutral comet assay performed as in B. (E) U2OS cells were treated with HU for the indicated hours and analyzed for the presence of DSBs using a neutral comet assay. The graph shows the percentage of cells with a comet tail moment >3.

Using pulsed-field gel electrophoresis (PFGE), DSBs are not detectable before 18–24 h after HU treatment (Petermann et al., 2010). However, we noticed that markers of DSBs (e.g., phosphorylated ATM, DNA-PK, and p53) were already present at earlier time points (4–8 h after addition of HU), although at a much lesser extent compared with cells treated with HU for 24 h (Fig. 1 B). Therefore, we used neutral comet assays, which detect single cells with DSBs, to determine whether some DSBs are generated before the 24-h time point of HU treatment. We found that a 3-h treatment with HU was enough to induce the appearance of some cells with a comet tail. The number of cells with tail and the tail moment calculated for the entire cell population increased with the time of HU treatment (Fig. 2 E; Fig. S2 E). However, when the tail moment was calculated only using the subpopulation of cells with a comet tail, less dramatic differences were observed at different times (Fig. S2 E, bottom right), showing that the amount of DSB per cell is not significantly different. These results suggest that the early appearance of DSB markers is due to DSB formation in a small population of cells, possibly the fraction that is in S phase at the time of HU treatment.

FBH1 confers sensitivity to HU

FBH1 is known to be recruited to ssDNA regions and increase ssDNA production (Fugger et al., 2009), so we also examined markers of ssDNA generation after HU treatment. In response to HU treatment, we observed an approximately twofold decrease in RPA2 bound to the chromatin in FBH1-depleted cells compared with control cells (Fig. 1 B). The differences detected by immunoblotting were not evident by immunofluorescence (Fig. 3 A), indicating that, although the same percentage of control and FBH1-depleted cells were positive for RPA at time 0, less RPA per cell was recruited to the chromatin upon FBH1 silencing. Similarly, when both control and FBH1-depleted cells

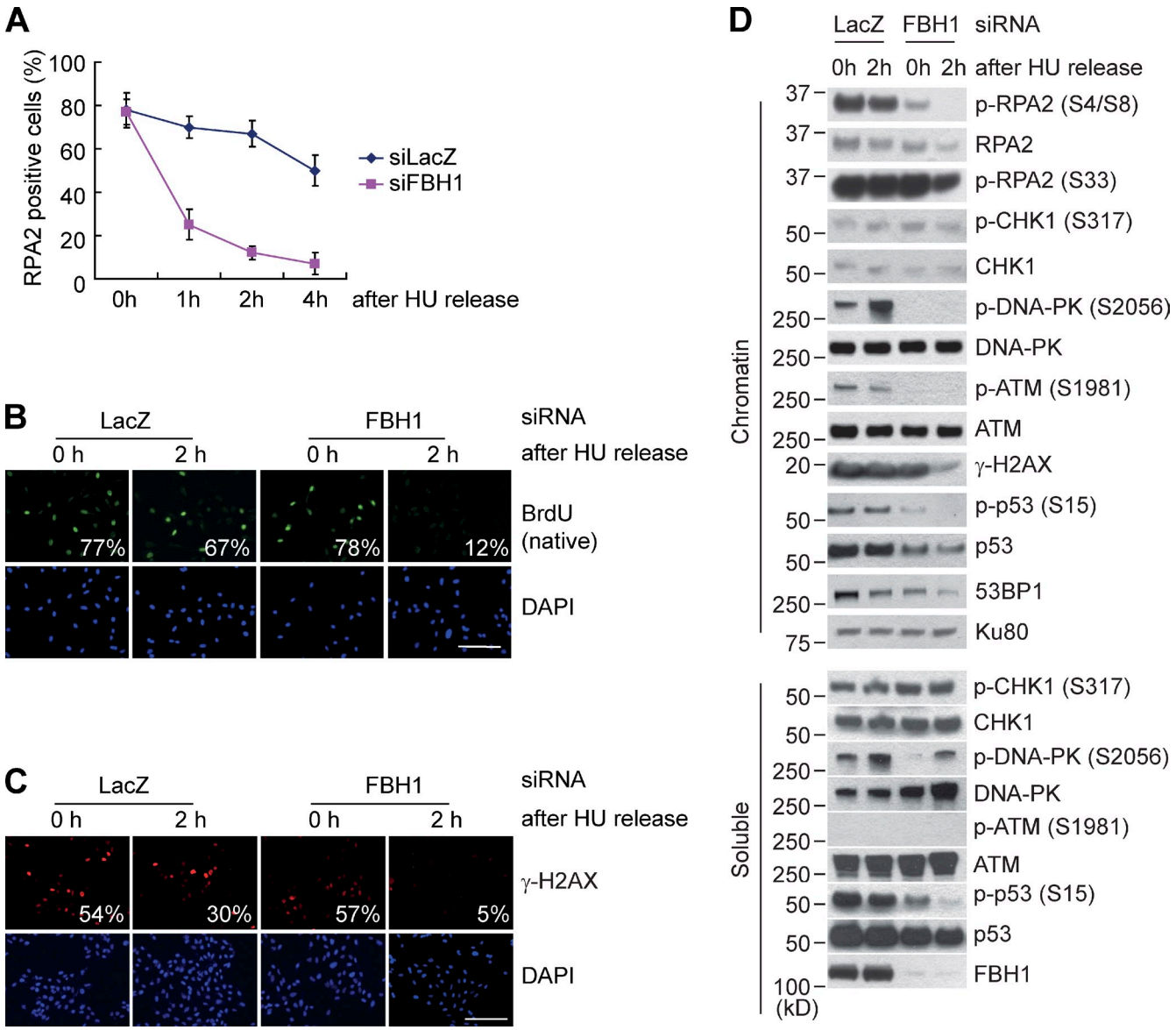

Figure 3. **FBH1-depleted cells quickly recover from DNA replication stress.** (A) U2OS cells were transfected with siRNAs to either LacZ or *FBH1* mRNA. After 48 h, cells were treated with HU for an additional 24 h, immediately fixed (0 h), or released for the indicated times into fresh medium. The number of p-RPA2(S4/S8)–positive cells from three different experiments was determined and plotted graphically (±SD). (B) U2OS cells were treated as in A, except they were also incubated with BrdU for 24 h before HU incubation. Cells were stained under native conditions, as indicated. (C) U2OS cells were treated as in A and stained as indicated. (D) U2OS cells were transfected with siRNAs to either LacZ or *FBH1* mRNA. After 48 h, cells were treated with HU for an additional 24 h (lanes 1 and 3) and released for 2 h into fresh medium (lanes 2 and 4). After harvesting, cells were fractionated into soluble and chromatin fractions, and lysates were immunoblotted as indicated.

were labeled with BrdU, incubated 24 h with HU, and stained with an antibody to BrdU under nondenaturing conditions (which allows BrdU detection only in ssDNA regions; Raderschall et al., 1999), no significant reduction in BrdU staining was detectable in FBH1 knockdown cells compared with control cells (Fig. 3 B; Fig. S3, A and B, time 0). We also immunostained cells for γ-H2AX, a phosphorylated form of H2AX produced by ATR, ATM, and DNA-PK. γ-H2AX accumulates quickly after HU treatment (before DSB induction) due to ATR activation and colocalizes with RPA foci, indicating that γ-H2AX marks areas flanking ssDNA regions (Petermann et al., 2010; Cleaver et al., 2011; Sirbu et al., 2011). Only after 18–24 h of treatment with HU a new phenotype (featuring much brighter, γ-H2AX–positive cells) appears, and these cells also stain for p-RPA2(S4/S8) (Fig. S3, C and D), suggesting that DSBs are present in these cells. 24 h after HU treatment, no significant differences between control and FBH1-depleted cells were observed in the percentage of γ-H2AX–positive cells and γ-H2AX foci; but the extremely bright γ-H2AX–positive cells were rarely observed in cells depleted of FBH1 (Fig. 3 C; Fig. S3 D), which is reflected in the limited amount of γ-H2AX present in the chromatin fraction at this time point (Fig. 1 B; Fig. S1 B).

In contrast to the modest effects observed after HU treatment, FBH1 silencing produced major effects in cells released from an HU block. In fact, although the percentage of EdU-positive cells (i.e., cells undergoing DNA synthesis) was

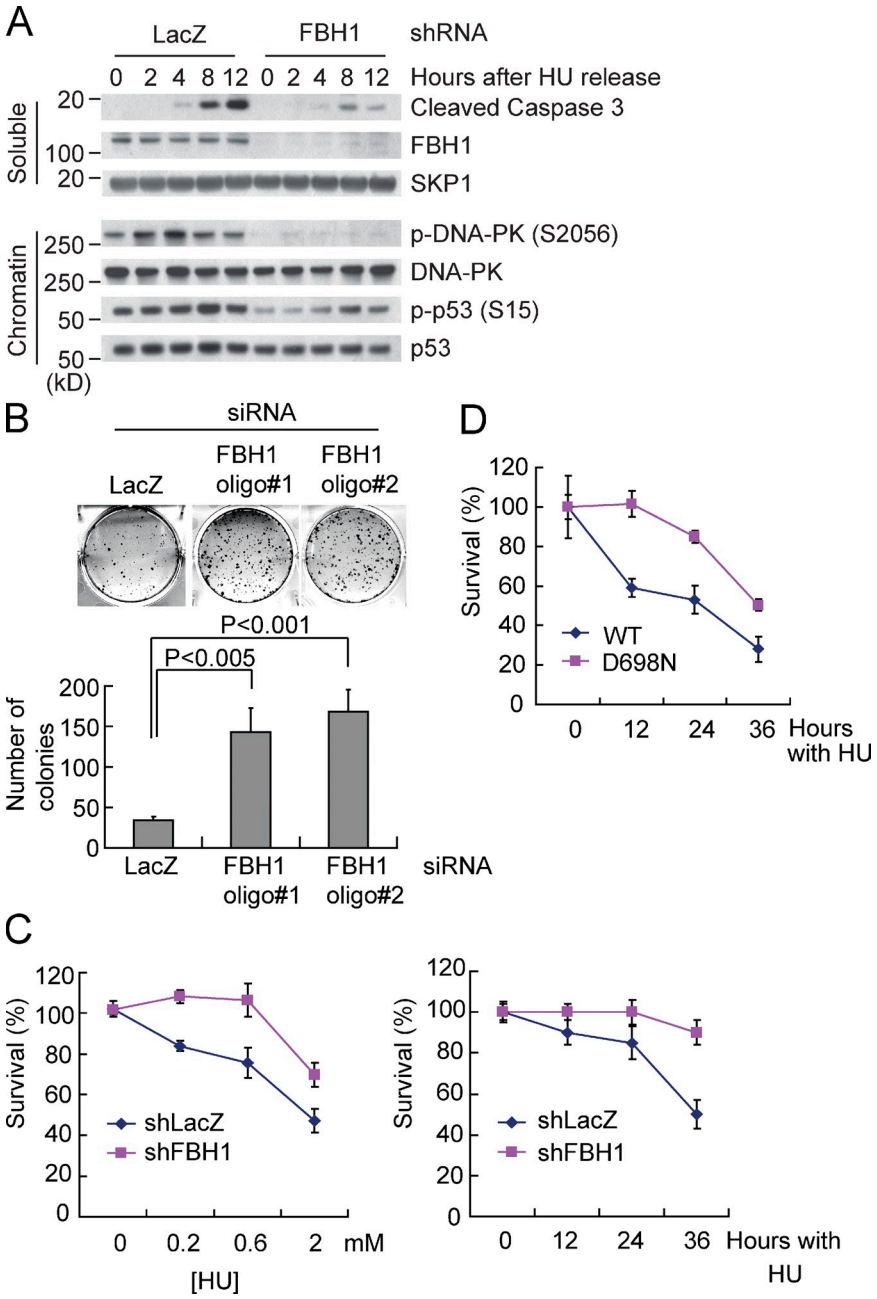

Figure 4. **FBH1 promotes apoptosis in response to replication stress.** (A) U2OS cells infected with lentiviruses encoding shRNAs to either LacZ or *FBH1* mRNA were treated with HU for an additional 36 h and released for the indicated times. Cells were harvested, and their lysates were immunoblotted as indicated. (B) U2OS cells were transfected with siRNAs to either LacZ or *FBH1* mRNA. After 48 h, cells were treated with HU for additional 72 h, released, cultured for an additional 10–15 d, and stained with crystal violet. The top images show representative examples. The bottom graph shows quantification of three independent experiments (±SD). P values were calculated by Student's *t* test. (C) U2OS cells infected with lentiviruses encoding shRNAs targeting either LacZ or *FBH1* mRNA were treated with the indicated concentrations of HU for 24 h (left) or with 0.2 mM HU for the indicated times, released, cultured for an additional 10–15 d, and stained with crystal violet. The graphs show quantification of three independent experiments (±SD). (D) U2OS cells stably infected with either an empty vector (EV), wild-type FBH1, or FBH1(D698N) were infected with lentiviruses encoding shRNAs to *FBH1* and treated with HU for the indicated times.

not affected (Fig. S3 E), RPA2 foci, BrdU positivity (under nondenaturing conditions), and γ-H2AX foci persisted after a release from the HU block in control cells, but they rapidly disappeared in FBH1 knockdown cells (Fig. 3, A–C). The effects on RPA2 and γ-H2AX were also confirmed by immunoblotting the chromatin fraction (Fig. 3 D). These results indicate that FBH1-depleted cells, having approximately twofold shorter ssDNA regions (as indicated by approximately twofold decrease in RPA2 bound to chromatin) and much fewer DSB, recover faster from DNA replication stress.

We also observed that, after release from a block in HU, control cells displayed cleaved Caspase 3, an established marker of apoptosis, but this response was strongly attenuated in FBH1-depleted cells (Fig. 4 A; Fig. S3 F), including $p53^{-/-}$ cells (Fig. S3 G). Accordingly, greater than four times more FBH1 knockdown cells than control cells survived 2 wks after release from a HU block, as judged by clonogenic survival assays (Fig. 4 B). This result was confirmed by a quantitative colony formation assay in which cells were exposed to different concentrations of HU or to the same concentration for different times (Fig. 4 C). Importantly, HU resistance was rescued by an siRNA-insensitive wild-type FBH1, but not an siRNA-insensitive FBH1(D698N) mutant (Fig. 4 D).

FBH1 contributes to DSB formation and apoptosis after UV irradiation in S phase

UV irradiation induces DNA photoproducts, mostly pyrimidine dimers (i.e., adjacent thymidines and cytosines linked covalently). The bulge created by these pyrimidine dimers is a physical block to DNA replication that, if not repaired, induces replication stress

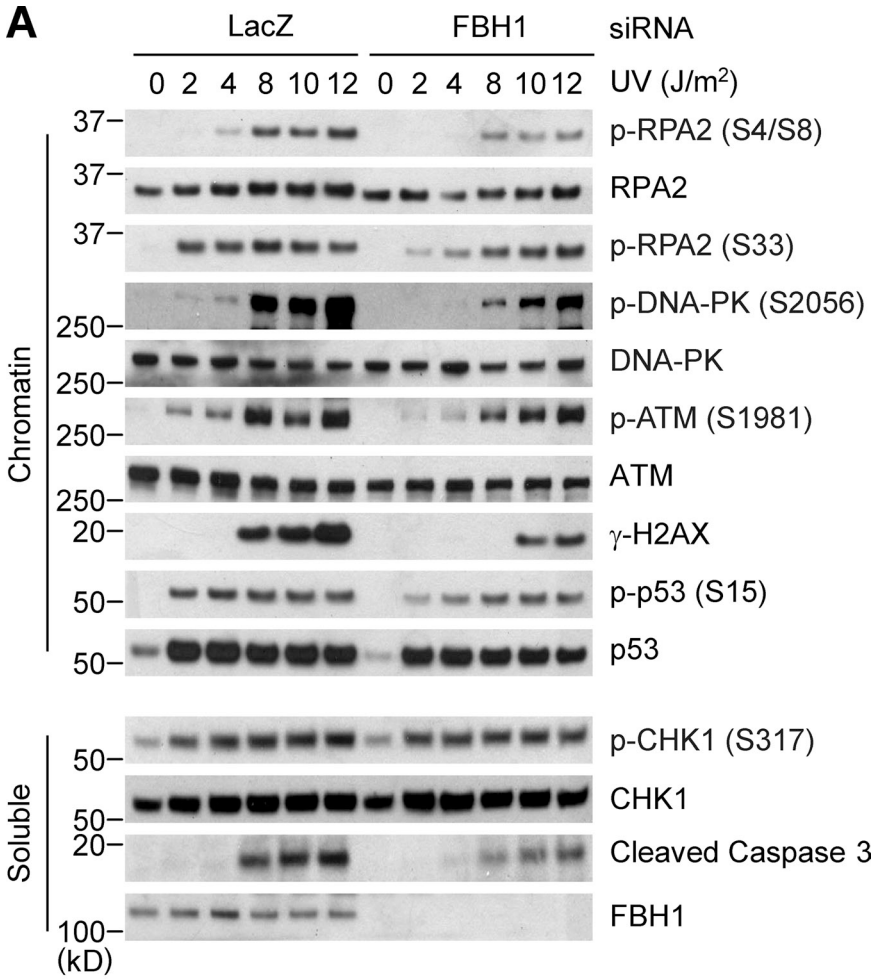

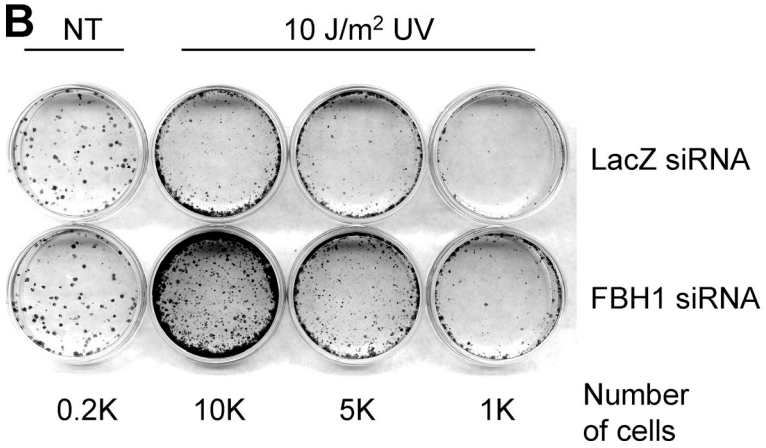

Figure 5. **FBH1 is required for the efficient activation of ATM and DNA-PK after DNA replication stress induced by UV.** (A) U2OS cells were transfected with siRNAs to either LacZ or *FBH1* mRNA. After 48 h, cells were accumulated at G1/S by a 16-h thymidine treatment. Cells were then released for 2 h, treated with the indicated ultraviolet (UV) doses, and left in culture for an additional 4 h. After harvesting, cells were fractionated into soluble and chromatin fractions, and lysates were immunoblotted as indicated. (B) U2OS cells, plated at different dilutions (decreasing from left to right), were treated as in A, except that after UV treatment they were cultured for 7 d and stained with crystal blue. NT, non-treated cells. Images show representative examples.

during S phase. Therefore, we investigated the role of FBH1 during the response to UV. U2OS cells were synchronized at G1/S by a single thymidine block and irradiated with different doses of UV 2 h after release from the block, when most cells were in S phase. We found that FBH1 silencing attenuated the DSB signaling response (i.e., reduced phosphorylation of DNA-PK, ATM, RPA2, p53, and H2AX) and reduced Caspase 3 cleavage (Fig. 5 A). In contrast, Chk1 phosphorylation was indistinguishable in control and FBH1-depleted cells. Finally, as shown by clonogenic survival assays, FBH1-depleted cells were less sensitive to UV irradiation (Fig. 5 B).

Conclusions and Implications

In *S. pombe*, Fbh1 acts as a Rad51 inhibitor to restrain HR, but in vertebrates, FBH1 plays either a minor or redundant role in restricting HR-dependent repair. Both in yeast and mammals, ssDNA accumulation is a precursor of DSB formation at collapsed replication forks (Saintigny et al., 2001; Petermann et al., 2010; Feng et al., 2011). When replication forks stall, the replicative DNA helicase is uncoupled from the DNA-polymerase machinery, resulting in significant lengths of ssDNA, which are covered by the RPA complex, activating the ATR-CHK1 signaling cascade. If the replication stress and ssDNA persist, DSBs

are generated and ATM and DNA-PK are activated, resulting in the phosphorylation of RPA2 and p53, and, eventually, cell death. We observed that this second phase of the response is attenuated in FBH1-depleted cells. Efficient double-strand breakage, activation of DNA-PK and ATM, and cell survival require FBH1 helicase activity. However, FBH1 does not affect the response to other forms of genotoxic stress in which DSBs are formed by means that do not require ssDNA intermediates.

We propose that, in higher organisms, FBH1 evolved as part of a mechanism to eliminate cells via apoptosis under conditions of chronic replication stress (e.g., promoted by UV or oncogenes), when too many forks have collapsed and restart efforts become futile. Elimination of these cells prevents oncogenic transformation due to damaged DNA and/or genome instability.

Materials and methods

Cell lines and drug treatments
HEK-293T cells were maintained in DMEM supplemented with 10% bovine serum (Invitrogen), and U2OS cells were maintained in DMEM supplemented with 10% fetal bovine serum (Invitrogen). Hydroxyurea, camptothecin, and neocarzinostatin were purchased from Sigma-Aldrich and used at concentrations of 2 mM, 1 µM, and 0.1 µg/ml, respectively.

UV treatment
Cells transfected with siRNA were incubated with 2 mM thymidine for 16 h and released into fresh media for 2 h to enrich the cells in S phase. Cells were irradiated with the indicated dosage of UVC (254 nm) with a spectrolinker (Spectronics).

Biochemical methods
For chromatin fractionation, cells were extracted with CSK buffer (D'Angiolella et al., 2010) for 5 min on ice and centrifuged for 3 min at 1,300 *g*. The insoluble pellets were digested with Turbo nuclease to generate the chromatin fraction. Each immunoblot was repeated at least three times (often in two different cell types) with virtually identical results. For immunoprecipitation, cell extracts were prepared using lysis buffer (50 mM Tris, pH 7.4, 150 mM NaCl, 2 mM EDTA, 10% glycerol, 0.5% NP-40, and protease inhibitors) followed by incubation with anti-FLAG antibody (M2; Sigma-Aldrich) for 2 h at 4°C. For immunoblotting, each sample was solubilized with SDS-sample buffer and boiled for 6 min at 95°C.

Immunofluorescence microscopy
Cells for immunofluorescence microscopy were cultured on round coverglasses in 24-well culture dishes. After drug treatments, cells were preextracted with CSK buffer (D'Angiolella et al., 2010) for 5 min, followed by fixation with 4% paraformaldehyde in PBS. Cells were then treated for 15 min with 3% BSA in 0.5% Triton X-100/PBS. Primary antibodies were incubated for 1 h, and secondary antibodies conjugated to either Alexa Fluor 488 or Alexa Fluor 555 were incubated for 30 min at room temperature in 3% BSA/0.1% Triton X-100/PBS. Coverglasses were mounted on slideglass using Pro-Long Gold anti-fading reagent (Invitrogen). Cells were stained with DAPI before mounting. Images were acquired with a microscope (40× objective lens, NA 0.75; Axiovert 200M; Carl Zeiss) equipped with a cooled CCD camera (Retiga 2000R; QImaging) and MetaMorph software (Molecular Devices). Images were cropped and prepared by Photoshop (Adobe) for the visualization.

Tandem affinity purification and mass spectrometry
HEK-293T cells were transiently transfected with FLAG-HA tagged plasmids using PEI (linear from Polysciences), and 24 h after transfection cell extracts were prepared in lysis buffer (50 mM Tris, pH 7.4, 150 mM NaCl, 1 mM EDTA, 25 mM NaF, and 0.5% NP-40) supplemented with protease and phosphatase inhibitors.

Protein complexes were immunopurified with anti-FLAG M2 agarose beads for 2 h at 4°C. After washing with lysis buffer, proteins were eluted twice by competition with FLAG peptide. In some cases, the eluate was then subjected to a second immunopurification with an anti-HA resin before elution by competition with HA peptide. Eluted fractions were TCA precipitated and the pellets were solubilized in Tris-HCl, pH 8.5, and 8 M urea; TCEP (Tris(2-carboxylethyl)-phosphine hydrochloride; Thermo Fisher Scientific) and CAM (Chloroacetamide; Sigma-Aldrich) were added to a final concentration of 5 mM and 10 mM, respectively. Protein suspensions were digested overnight at 37°C using Endoproteinase Lys-C at 1:50 wt/wt (Roche). Samples were brought to a final concentration of 2 M urea and 2 mM $CaCl_2$ before performing a second overnight digestion at 37°C using Trypsin (Promega) at 1:100 wt/wt. Formic acid (5% final) was added to stop the reactions. Samples were loaded on split-triple-phase fused-silica microcapillary columns (MacCoss et al., 2002) and placed in-line with linear ion trap mass spectrometers (LTQ; Thermo Fisher Scientific), coupled with quaternary 1100 or 1200 series HPLCs (Agilent Technologies). A fully automated 10-step chromatography run (for a total of 20 h) was performed for each sample (Washburn et al., 2001; Florens and Washburn, 2006) enabling dynamic exclusion for 120 s. Tandem mass (MS/MS) spectra were interpreted using SEQUEST software (Eng et al., 1994) against a database of 59,070 sequences that consist of 29,375 different human proteins (NCBI's 2010–11-22 release), 160 usual contaminants and, to estimate false discovery rates (FDRs), 29,535 randomized amino acid sequences derived from the 29,375 different human proteins. Peptide/spectrum matches were sorted and selected using DTASelect software (Tabb et al., 2002) and peptides from multiple runs were compared using CONTRAST. Spectra/peptide matches were retained only if they had a DeltCn of at least 0.08 and a minimum XCorr of 1.8 for singly, 2.5 for doubly, and 3.5 for triply charged spectra. Peptides had to be fully tryptic and at least seven amino acids long, and positive identification required two unique peptides or one peptide with two independent spectra. The FDRs at the protein and peptide levels were 1.1% ± 1 and 0.12% ± 0.13, respectively. To estimate relative protein levels, distributed normalized spectral abundance factors (dNSAFs) were calculated for each detected protein, as described in Zhang et al. (2010). The dNSAF values account for differences in protein length and prevent redundant spectral assignment, allowing for the comparison of the relative spectral abundance of proteins across various preparations, and are primarily based on distribution of shared spectral counts among isoforms.

Plasmids, siRNA, and shRNA
FBH1 mutants were generated using the QuikChange Site-Directed Mutagenesis kit (Agilent Technologies). Both wild-type and mutants were subcloned into the pBabe retroviral vector. All cDNAs were subsequently sequenced. ON-Target siRNAs to FBH1 were purchased from Thermo Fisher Scientific. The production of lentivirus-encoding shRNAs that target human FBH1 was described previously (Busino et al., 2007). The target sequence used to knockdown human FBH1 is 5′-GCAATAGGATTCACTACAA-3′.

Antibodies
Mouse monoclonal antibodies were from EMD Millipore (RPA2 and γ-H2AX), Genetex (RPA3), Sigma-Aldrich (anti-FLAG M2), Covance (anti-HA), Santa Cruz Biotechnology, Inc. (PCNA), Abcam (phospho-DNA-PK [S2056] and 53BP1), Invitrogen (PARP1), and Cell Signaling Technology (phospho-S1981 ATM). Rabbit polyclonal antibodies were from Cell Signaling Technology (phosho-CHK1 [Ser317], Caspase-3), Invitrogen (CUL1 and SKP1), and Bethyl Laboratories, Inc. (phospho-RPA2 [S4S8] and phopho-RPA2 [S33]). The FBH1 antibody was generated using a GST fusion to the N terminus of FBH1 (Yenzyme).

Transient transfections and retroviral infection
HEK-293T cells were cotransfected with target retroviral plamid, VSVg, and Gag/Pol using PEI. 24 h after transfection, virus-containing media were harvested and supplemented with 8 mg/ml polybrene (Sigma-Aldrich). Cells were infected by incubating cells overnight with the viral supernatant. Each infection was performed twice. siRNAs were transfected into U2OS cells using HiPerfect reagent (QIAGEN) according to the manufacturer's guidelines.

Comet assay
Comet assay was performed according to the manufacturer's instructions (Trevigen). In brief, cells were harvested after drug treatments, mixed with low melting agarose, and allowed to be solidified on slides. Cells were incubated in lysis buffer, before incubation in neutralization buffer. Slides were washed twice with Tris-borate-EDTA, placed in a horizontal electrophoresis apparatus, and voltage (12 V) was applied for 10 min. Slides were incubated in 70% ethanol and dried at room temperature overnight. Finally, slides were stained for 10 min with SYBR Green 1 (Molecular Probes) and washed once with TBE. All procedures were performed in the dark to prevent DNA damage. At least 300 cells were counted in each condition over three independent experiments. Experiments were quantified using CometScore software (TriTek Corp.).

Clonogenic assay

Cells were transfected with siRNAs to FBH1 or LacZ, and after 48 h they were replated and incubated with HU for 48 h. Cells were then released into fresh media for another 7–10 d to allow colony formation. For UV treatment, cells were incubated with thymidine for 16 h, released for 2 h, irradiated with 10 J/m^2 of UVC, and incubated with fresh media for another 7–10 d to allow colony formation. The colonies were washed with PBS and stained with Crystal Violet (Sigma-Aldrich).

Online supplemental material

Fig. S1 shows additional data illustrating that FBH1 promotes the activation of ATM and DNA-PK and the phosphorylation of RPA2 on Ser4 and Ser8 after DNA replication stress induced by HU treatment. Fig. S2 shows additional data demonstrating that the helicase domain of FBH1 is required for phosphorylation of RPA2 on Ser4 and Ser8 after HU treatment. Fig. S3 shows additional data demonstrating that FBH1 confers sensitivity to HU. Tables S1 and S2 show mass spectrometry analysis of FBH1 immunopurifications. Online supplemental material is available at http://www.jcb.org/cgi/content/full/jcb.201209002/DC1.

The authors thank M. Aladjem, J. Borowiec, G. Draetta, T. Heffernan, J. Marszalek, and D. Rucando for reagents; J. Borowiec, V. Costanzo, D. Durocher, M. Foiani, H. Klein, J. Lukas, and J. R. Skaar for critical reading of the manuscript; and C. Sørensen and J. Bartek for sharing unpublished results. M. Pagano and Y.-T. Jeong are grateful to T.M. Thor and S.O. Hong, respectively, for continuous support.

This work was funded by grants from the National Institutes of Health (R01-GM057587, R37-CA076584, and R21-CA161108 to M. Pagano; R03-TW009040 to M. Rossi; R01-ES015632 to P. Sung; and R01-GM045751 to C.L. Schildkraut), a fellowship from the Korean National Research Foundation (no. KRF-2007-357-C00082 to Y.-T. Jeong), and an Empire State Stem Cell Fund, New York State (contract C024348 to C.L. Schildkraut). A. Saraf, L. Florens, and M.P. Washburn are supported by the Stowers Institute for Medical Research. M. Pagano is an Investigator with the Howard Hughes Medical Institute.

Submitted: 3 September 2012
Accepted: 21 December 2012

References

Barber, L.J., J.L. Youds, J.D. Ward, M.J. McIlwraith, N.J. O'Neil, M.I. Petalcorin, J.S. Martin, S.J. Collis, S.B. Cantor, M. Auclair, et al. 2008. RTEL1 maintains genomic stability by suppressing homologous recombination. *Cell*. 135:261–271. http://dx.doi.org/10.1016/j.cell.2008.08.016

Binz, S.K., A.M. Sheehan, and M.S. Wold. 2004. Replication protein A phosphorylation and the cellular response to DNA damage. *DNA Repair (Amst.)*. 3:1015–1024. http://dx.doi.org/10.1016/j.dnarep.2004.03.028

Busino, L., F. Bassermann, A. Maiolica, C. Lee, P.M. Nolan, S.I. Godinho, G.F. Draetta, and M. Pagano. 2007. SCFFbxl3 controls the oscillation of the circadian clock by directing the degradation of cryptochrome proteins. *Science*. 316:900–904. http://dx.doi.org/10.1126/science.1141194

Chiolo, I., M. Saponaro, A. Baryshnikova, J.H. Kim, Y.S. Seo, and G. Liberi. 2007. The human F-Box DNA helicase FBH1 faces *Saccharomyces cerevisiae* Srs2 and postreplication repair pathway roles. *Mol. Cell. Biol.* 27:7439–7450. http://dx.doi.org/10.1128/MCB.00963-07

Chu, W.K., and I.D. Hickson. 2009. RecQ helicases: multifunctional genome caretakers. *Nat. Rev. Cancer*. 9:644–654. http://dx.doi.org/10.1038/nrc2682

Ciccia, A., and S.J. Elledge. 2010. The DNA damage response: making it safe to play with knives. *Mol. Cell*. 40:179–204. http://dx.doi.org/10.1016/j.molcel.2010.09.019

Cleaver, J.E., L. Feeney, and I. Revet. 2011. Phosphorylated H2Ax is not an unambiguous marker for DNA double-strand breaks. *Cell Cycle*. 10:3223–3224. http://dx.doi.org/10.4161/cc.10.19.17448

D'Angiolella, V., V. Donato, S. Vijayakumar, A. Saraf, L. Florens, M.P. Washburn, B. Dynlacht, and M. Pagano. 2010. SCF(Cyclin F) controls centrosome homeostasis and mitotic fidelity through CP110 degradation. *Nature*. 466:138–142. http://dx.doi.org/10.1038/nature09140

Eng, J., A.L. McCormack, and J.R. Yates III. 1994. An approach to correlate tandem mass spectral data of peptides with amino acid sequences in a protein database. *J. Amer. Mass Spectrom.* 5:976–989. http://dx.doi.org/10.1016/1044-0305(94)80016-2

Feng, W., S. DiRienzi, M. Raghuraman, and B. Brewer. 2011. Replication stress-induced chromosome breakage is correlated with replication fork progression and is preceded by single-stranded DNA formation. *Genes, Genomes. Genetics*. 1:327–335.

Florens, L., and M.P. Washburn. 2006. Proteomic analysis by multidimensional protein identification technology. *Methods Mol. Biol.* 328:159–175.

Fugger, K., M. Mistrik, J.R. Danielsen, C. Dinant, J. Falck, J. Bartek, J. Lukas, and N. Mailand. 2009. Human Fbh1 helicase contributes to genome maintenance via pro- and anti-recombinase activities. *J. Cell Biol.* 186:655–663. http://dx.doi.org/10.1083/jcb.200812138

Kim, J., J.H. Kim, S.H. Lee, D.H. Kim, H.Y. Kang, S.H. Bae, Z.Q. Pan, and Y.S. Seo. 2002. The novel human DNA helicase hFBH1 is an F-box protein. *J. Biol. Chem.* 277:24530–24537. http://dx.doi.org/10.1074/jbc.M201612200

Kim, J.H., J. Kim, D.H. Kim, G.H. Ryu, S.H. Bae, and Y.S. Seo. 2004. SCFhFBH1 can act as helicase and E3 ubiquitin ligase. *Nucleic Acids Res.* 32:2287–2297. http://dx.doi.org/10.1093/nar/gkh534

Kohzaki, M., A. Hatanaka, E. Sonoda, M. Yamazoe, K. Kikuchi, N. Vu Trung, D. Szüts, J.E. Sale, H. Shinagawa, M. Watanabe, and S. Takeda. 2007. Cooperative roles of vertebrate Fbh1 and Blm DNA helicases in avoidance of crossovers during recombination initiated by replication fork collapse. *Mol. Cell. Biol.* 27:2812–2820. http://dx.doi.org/10.1128/MCB.02043-06

Laulier, C., A. Cheng, N. Huang, and J.M. Stark. 2010. Mammalian Fbh1 is important to restore normal mitotic progression following decatenation stress. *DNA Repair (Amst.)*. 9:708–717. http://dx.doi.org/10.1016/j.dnarep.2010.03.011

Lawrence, C.L., N. Jones, and C.R. Wilkinson. 2009. Stress-induced phosphorylation of *S. pombe* Atf1 abrogates its interaction with F box protein Fbh1. *Curr. Biol.* 19:1907–1911. http://dx.doi.org/10.1016/j.cub.2009.09.044

MacCoss, M.J., W.H. McDonald, A. Saraf, R. Sadygov, J.M. Clark, J.J. Tasto, K.L. Gould, D. Wolters, M. Washburn, A. Weiss, et al. 2002. Shotgun identification of protein modifications from protein complexes and lens tissue. *Proc. Natl. Acad. Sci. USA*. 99:7900–7905. http://dx.doi.org/10.1073/pnas.122231399

Manthey, K.C., S. Opiyo, J.G. Glanzer, D. Dimitrova, J. Elliott, and G.G. Oakley. 2007. NBS1 mediates ATR-dependent RPA hyperphosphorylation following replication-fork stall and collapse. *J. Cell Sci.* 120:4221–4229. http://dx.doi.org/10.1242/jcs.004580

Moldovan, G.L., D. Dejsuphong, M.I. Petalcorin, K. Hofmann, S. Takeda, S.J. Boulton, and A.D. D'Andrea. 2012. Inhibition of homologous recombination by the PCNA-interacting protein PARI. *Mol. Cell*. 45:75–86. http://dx.doi.org/10.1016/j.molcel.2011.11.010

Morishita, T., F. Furukawa, C. Sakaguchi, T. Toda, A.M. Carr, H. Iwasaki, and H. Shinagawa. 2005. Role of the *Schizosaccharomyces pombe* F-Box DNA helicase in processing recombination intermediates. *Mol. Cell. Biol.* 25:8074–8083. http://dx.doi.org/10.1128/MCB.25.18.8074-8083.2005

Osman, F., J. Dixon, A.R. Barr, and M.C. Whitby. 2005. The F-Box DNA helicase Fbh1 prevents Rhp51-dependent recombination without mediator proteins. *Mol. Cell. Biol.* 25:8084–8096. http://dx.doi.org/10.1128/MCB.25.18.8084-8096.2005

Park, J.S., E. Choi, S.H. Lee, C. Lee, and Y.S. Seo. 1997. A DNA helicase from *Schizosaccharomyces pombe* stimulated by single-stranded DNA-binding protein at low ATP concentration. *J. Biol. Chem.* 272:18910–18919. http://dx.doi.org/10.1074/jbc.272.30.18910

Petermann, E., M.L. Orta, N. Issaeva, N. Schultz, and T. Helleday. 2010. Hydroxyurea-stalled replication forks become progressively inactivated and require two different RAD51-mediated pathways for restart and repair. *Mol. Cell*. 37:492–502. http://dx.doi.org/10.1016/j.molcel.2010.01.021

Raderschall, E., E.I. Golub, and T. Haaf. 1999. Nuclear foci of mammalian recombination proteins are located at single-stranded DNA regions formed after DNA damage. *Proc. Natl. Acad. Sci. USA*. 96:1921–1926. http://dx.doi.org/10.1073/pnas.96.5.1921

Saintigny, Y., F. Delacôte, G. Varès, F. Petitot, S. Lambert, D. Averbeck, and B.S. Lopez. 2001. Characterization of homologous recombination induced by replication inhibition in mammalian cells. *EMBO J.* 20:3861–3870. http://dx.doi.org/10.1093/emboj/20.14.3861

Sakaguchi, C., T. Morishita, H. Shinagawa, and T. Hishida. 2008. Essential and distinct roles of the F-box and helicase domains of Fbh1 in DNA damage repair. *BMC Mol. Biol.* 9:27. http://dx.doi.org/10.1186/1471-2199-9-27

Sirbu, B.M., F.B. Couch, J.T. Feigerle, S. Bhaskara, S.W. Hiebert, and D. Cortez. 2011. Analysis of protein dynamics at active, stalled, and collapsed replication forks. *Genes Dev.* 25:1320–1327. http://dx.doi.org/10.1101/gad.2053211

Tabb, D.L., W.H. McDonald, and J.R. Yates III. 2002. DTASelect and Contrast: tools for assembling and comparing protein identifications from shotgun proteomics. *J. Proteome Res.* 1:21–26. http://dx.doi.org/10.1021/pr015504q

Washburn, M.P., D. Wolters, and J.R. Yates III. 2001. Large-scale analysis of the yeast proteome by multidimensional protein identification technology. *Nat. Biotechnol.* 19:242–247. http://dx.doi.org/10.1038/85686

Zhang, Y., Z. Wen, M.P. Washburn, and L. Florens. 2010. Refinements to label free proteome quantitation: how to deal with peptides shared by multiple proteins. *Anal. Chem.* 82:2272–2281. http://dx.doi.org/10.1021/ac9023999